

Scenarios for sea level on the Finnish coast

Milla M. Johansson, Kimmo K. Kahma, Hanna Boman
and Jouko Launiainen

Finnish Institute of Marine Research, P.O. Box 33, FIN-00931 Helsinki, Finland

Johansson, M. M., Kahma, K. K., Boman, H. & Launiainen, J. 2004: Scenarios for sea level on the Finnish coast. *Boreal Env. Res.* 9: 153–166.

The linkage between global climate change and sea level on the Finnish coast was studied. Scenarios were calculated for the long-term mean sea level in the future, based on the global change scenarios given by the Intergovernmental Panel on Climate Change. The effects of global mean sea level, local land uplift and the water balance of the Baltic Sea were taken into account. The effect of the water balance was estimated with the North Atlantic Oscillation (NAO) index. In most cases the rise in water level is expected to balance the land uplift in the Gulf of Finland, and the past declining trend of the relative sea level is not expected to continue. In the Gulf of Bothnia, the stronger land uplift rate still results in a fall of the relative mean sea level in the future. The uncertainties in the scenarios are large. Scenarios for the intra-annual variability of the sea level were constructed by extrapolating the 20th century trends of increasing variability.

Introduction

The behaviour of the sea level on the Finnish coast was studied as a part of the project FIGARE/FINSKEN. The purpose was to examine the linkage between the global climate change and the sea level on the Finnish coast, and to present scenarios of future sea levels.

In this paper, we summarize the sea level studies made at the Finnish Institute of Marine Research (FIMR) during the FINSKEN project. Trends in short-term sea level variability during the 20th century were studied by Johansson *et al.* (2001). Johansson *et al.* (2003) studied the observed long-term variability of the sea level and the factors affecting it, and developed a method for calculating estimates of the long-term mean sea level. Based on the results of these studies, scenarios for the sea level are constructed in this paper.

The sea level scenarios for the Finnish coast are based on the global scenarios presented by the Intergovernmental Panel on Climate Change (IPCC) in the Third Assessment Report (IPCC 2001). Several storylines of future global socio-economic development are defined by the IPCC, resulting in different scenarios of greenhouse gas and aerosol emissions (the SRES scenarios, Nakićenović *et al.* 2000, Carter *et al.* 2004). The SRES emission scenarios are used to estimate changes in atmospheric composition, changes in radiative forcing of the climate, changes in the global mean temperature, and, finally, scenarios of the global mean sea level.

We studied six different SRES emission scenarios designated as A1B, A1T, A1FI, A2, B1 and B2. The scenario A1 describes a world with very rapid economic growth and rapid introduction of new technologies. It is divided into three different scenarios based on the energy sources

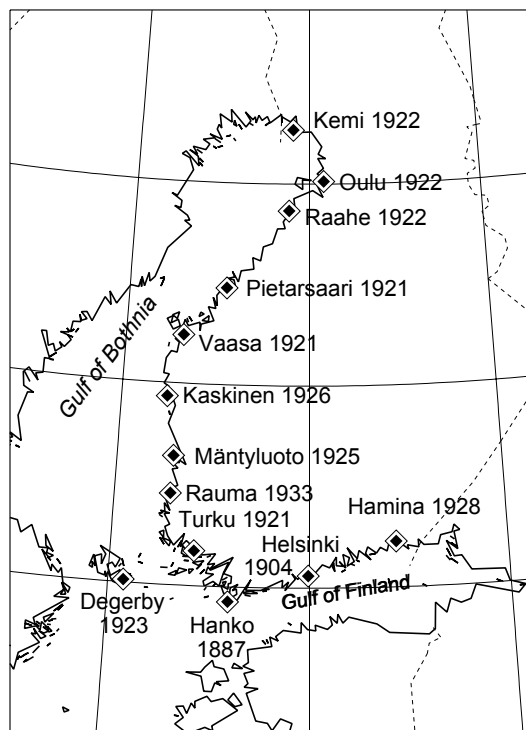


Fig. 1. Locations and years of establishment of the Finnish tide gauges.

mainly utilized: the fossil-intensive A1FI scenario, the non-fossil based A1T scenario, and the balance across all sources, A1B. The A2 scenario describes a heterogeneous world with regionally oriented economic development and fragmented and slow technological change. The B1 scenario describes a convergent world with rapid change in economic structures toward a service and information economy. The B2 scenario describes a world in which emphasis is on local solutions to economic, social and environmental sustainability (IPCC 2001).

Finnish sea level data

This study is based on sea level observations from the 13 Finnish tide gauges (Fig. 1). The longest sea level time series, at Hango, starts in 1887, and the shortest one, at Rauma, starts in 1933. The observation series cover at least 80 years at most tide gauges, and are suitable for studies of the long-term changes.

We used observations at 4-hour intervals, measured in relation to a bedrock-bound reference level, the latter defined separately for each tide gauge (Lisitzin 1966). For various reasons, there are gaps in the observation time series, ranging from single hours up to several months. The gaps were patched by interpolating the sea level values using observations at the adjacent tide gauges. The interpolating is a generally reliable method in the case of sea level observations. For a more detailed presentation of the equipment used, problems discovered, and the corrections applied to the sea level observations, *see* Johansson *et al.* (2001).

Mean sea level

Observed trends in mean sea level during the 20th century

While the annual mean of sea level varies considerably from year to year, a declining trend was seen up to 1980 in all the Finnish sea level time series (Fig. 2). The magnitude of this rather linear decrease depends on the location; it was greatest at Vaasa in the Gulf of Bothnia, and smallest in the inner part of the Gulf of Finland, at Hamina.

The linear trend has been previously analysed, and estimates for the long-term mean sea level calculated (Lisitzin 1964, Vermeer *et al.* 1988, Johansson *et al.* 2003). During the last two decades of the 20th century the sea level no longer followed the steady linear trend (Fig. 2). The long-term mean sea level was then on average 5 cm higher than the historical linear trend would suggest. This is supposed to be due to changes in the Baltic Sea water balance (Johansson *et al.* 2003).

Factors affecting the mean sea level

Rise in global mean sea level and land uplift

The two most important factors affecting the mean sea level on the Finnish coast are the land uplift and the rise in the global mean sea level. They both cause a long-term, trend-like change

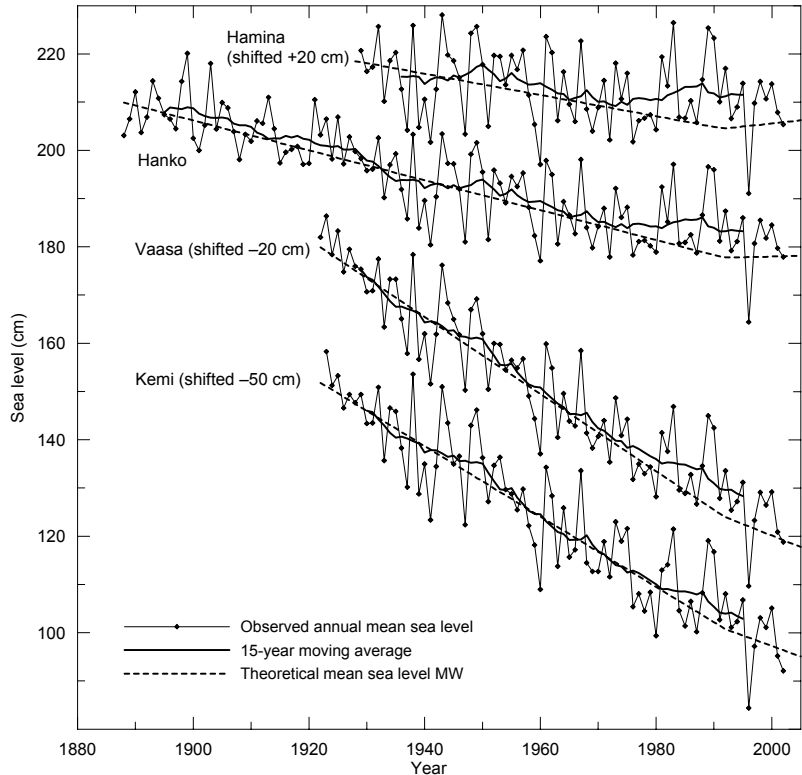


Fig. 2. Observed annual mean sea level at selected Finnish tide gauges, and the 15-year moving averages. The theoretical mean sea level is a forecast of the time-dependent expectation value of the long-term mean sea level. The sea levels are given in relation to the bedrock-bound reference levels (see text). The vertical scale is for Hanko, other stations have been shifted for clarity.

in sea level — the former a falling one and the latter a rising one. The balance between these two determines whether the sea level is generally rising or falling in relation to the bedrock.

The global mean sea level rose linearly during the 20th century, within the limits of observation accuracy. The current estimate for the rise amounts to $1\text{--}2\text{ mm yr}^{-1}$ (IPCC 2001). In the future, the linear behaviour of the global mean sea level might change. IPCC (2001) presents scenarios for the global mean sea level in the 21st century, based on the SRES emission scenarios (Nakićenović *et al.* 2000). According to these scenarios (Fig. 3), the sea level will rise 9–88 cm during 1990–2100. The rise in the global mean sea level results from the rise of the temperature. This temperature rise affects sea level mainly in two ways; thermal expansion of seawater and melting of land-based glaciers. However, increasing precipitation — caused by the rising temperature — might also lead to the accumulation of more ice on the Antarctic ice sheets, which would act to reduce the sea level.

In this study, we assume that the rise in the

global mean sea level is equal everywhere. In fact, the large-scale mean sea level affecting the Baltic Sea is better represented by the mean sea level in the North Sea area, outside the Baltic entrance, which might deviate from the global mean sea level. The observations from the European tide gauges (Gornitz 1995) might represent this kind of mean sea level. These observations result in an estimate of 1.5 mm yr^{-1} for the mean sea level rise during the 20th century, which is in accordance with the IPCC estimate.

The land uplift, caused by postglacial rebound, proceeds linearly on a time scale of a couple of hundred years, and within the accuracy limits sufficient for this study. The rate of land uplift varies greatly along the Finnish coastline, being strongest around Vaasa and weakest on the coast of the Gulf of Finland.

In the Finnish sea level observation period 1887–2002, the linear effects of land uplift and global mean sea level rise can be combined together to form a relative land uplift rate

$$u_{ri} = u_{ai} - G \quad (1)$$

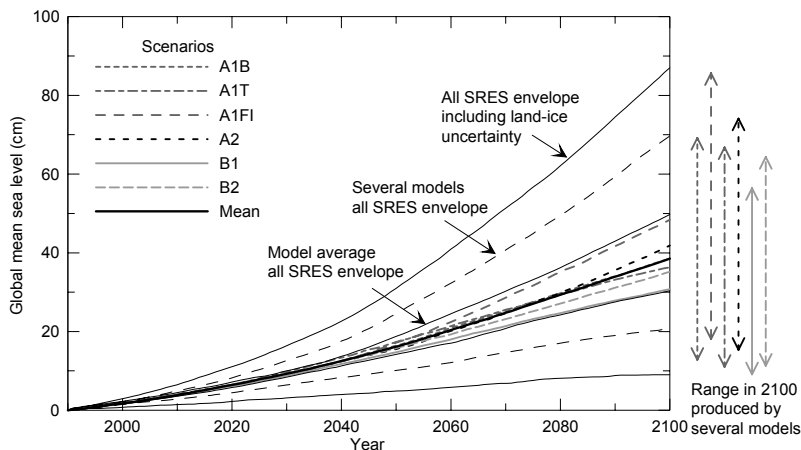


Fig. 3. Scenarios for the global mean sea level rise in the 21st century, according to the different SRES emission scenarios (IPCC 2001). The “several models all SRES envelope” denotes the scatter of all models for the full range of 35 SRES scenarios. The “model average all SRES envelope” shows the range of the average of the models for all 35 scenarios. The “all SRES envelope including land-ice uncertainty” shows the range of all models and scenarios including uncertainty in land-ice changes, permafrost changes and sediment deposition.

where u_{ri} is the relative land uplift rate, u_{ai} is the absolute land uplift rate (subscript i henceforth refers to location of the gauges; *see* Table 1), and G is the rate of the global mean sea level rise. After the effect of the water balance is corrected for in the sea level observation time series, an estimate for the relative land uplift can be calculated by linear regression (Johansson *et al.* 2003). At the Finnish tide gauge locations, these rates vary between 1.6 mm yr^{-1} and 7.5

mm yr^{-1} (Table 1), the 95% error margin being of the order of $0.4\text{--}0.6 \text{ mm yr}^{-1}$. The absolute land uplift rates were obtained by adding the global mean sea level rise rate of $1.5 \pm 0.5 \text{ mm yr}^{-1}$ to the relative land uplift. These absolute land uplift rates are the same for the 21st century as for the 20th century.

Table 1. The land uplift rates at the Finnish tide gauges, together with the 95% probability error margin. The absolute land uplift rates were calculated by combining the relative land uplift rates and the global mean sea level rise (*see* the text).

Tide gauge	Relative land uplift u_{ri} (mm yr^{-1})	Absolute land uplift u_{ai} (mm yr^{-1})
Kemi	7.20 ± 0.55	8.70 ± 0.74
Oulu	6.87 ± 0.54	8.37 ± 0.73
Raahe	7.22 ± 0.52	8.72 ± 0.72
Pietarsaari	7.31 ± 0.50	8.81 ± 0.71
Vaasa	7.46 ± 0.44	8.96 ± 0.67
Kaskinen	6.99 ± 0.47	8.49 ± 0.69
Mäntyluoto	6.07 ± 0.44	7.57 ± 0.67
Rauma	5.35 ± 0.49	6.85 ± 0.70
Turku	3.94 ± 0.43	5.44 ± 0.66
Degerby	4.13 ± 0.44	5.63 ± 0.66
Hanko	2.63 ± 0.42	4.13 ± 0.65
Helsinki	2.01 ± 0.43	3.51 ± 0.66
Hamina	1.62 ± 0.52	3.12 ± 0.72

Baltic Sea water balance and correlation with the NAO index

The total water volume inside the semi-enclosed Baltic Sea can vary by some 365 km^3 , which corresponds to variation in the sea level of approximately one meter (Johansson *et al.* 2003). These variations in the water balance do not even out on an annual time scale: they explain most of the year-to-year variability of annual mean sea levels, and they affect even the 15-year moving averages of sea level (Fig. 2).

The variations in the water balance are mainly caused by inflow and outflow of water through the Danish Straits. This exchange is controlled by meteorological conditions, such as wind and air pressure over the Strait area. In particular, westerly winds push water into the Baltic Sea. The Baltic Sea level is affected on time scales longer than days, typically about two weeks, because the narrow straits have a limited flow capacity.

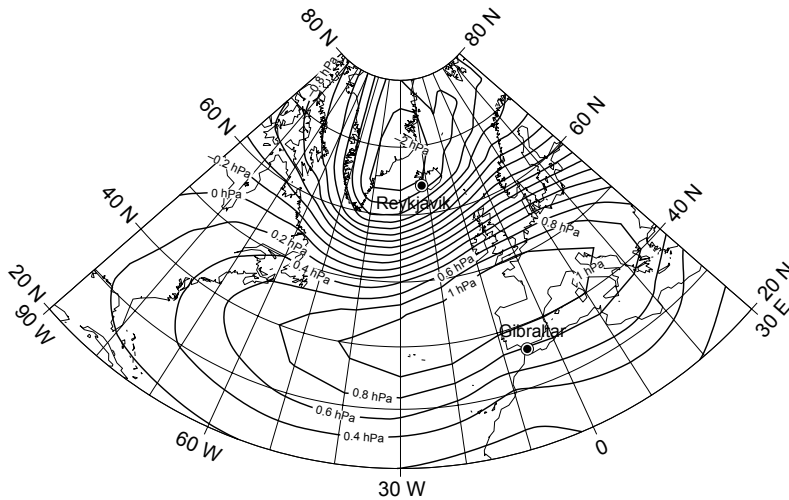


Fig. 4. Air pressure anomalies associated with the leading principal component obtained from an EOF analysis of the time series of winter (December–March) mean anomalies of the observed sea level pressure in 1873–2000. To obtain the physical units (hPa), the anomaly field was calculated as a “regression map” by regressing the leading principal component time series to the yearly anomaly fields (as in Thompson and Wallace 2000). The observation sites used for the calculation of the station-based NAO index are marked with circles.

Other factors contributing to the water balance are river run-off, precipitation and evaporation, but the net effect of these tends to be minor as compared with the effect of the water exchange through the straits. The effect of river run-off is further discussed in Vermeer *et al.* (1988). Mean temperature and salinity of the Baltic Sea water also have a minor effect on the sea level.

The sea level variability along the Finnish coast correlates with the North Atlantic Oscillation (NAO) index (Kahma 1999, Johansson *et al.* 2003). There are several different ways to define the NAO index. In this study, we use indices defined for the winter period December–March, since these turned out to be the most suitable for our purposes.

The station-based NAO index is defined as a difference between normalized air pressure anomalies at Gibraltar and south-west Iceland, averaged over the winter period (Jones *et al.* 1997). When considering climate models, as is the case below, and longer time scales extending to the future, an air pressure gradient defined from two points is not optimal, since the location of the pressure centres forming the North Atlantic Oscillation phenomenon may vary between models and also change in time. Since the index should represent a large-scale oscillation, a better approach is to calculate it from a spatially wider

pressure field. We used observed mean sea level pressures over the North Atlantic (20°N–80°N and 90°W–30°E), on a grid with 5° latitudinal and 10° longitudinal resolution (Basnett and Parker 1997), and calculated the NAO index as the amplitude of the leading principal component, obtained from an empirical orthogonal function (EOF) analysis of the December–March average pressure fields in 1873–2000. The anomalies of the observed pressure field associated with the leading principal component are shown in Fig. 4.

The mutual correlation between the station-based NAO index and the leading principal component is good, the coefficient of determination (R^2) being 0.81. Both of these indices correlate significantly with the annual mean sea levels on the Finnish coast (Table 2). Prior to calculating the correlations, linear trends were removed from both the annual mean sea level and the NAO index time series. The coefficients of determination (R^2) vary between 0.33 and 0.46. Since neither of the correlating variables is a direct cause of the other one — both can be considered as being affected by a common background process — the regression coefficients were calculated using the maximum likelihood effective variance method. The relative uncertainties in the variables were approximated by the standard deviations of the respective time series.

This significant correlation permits an estimation of the Baltic Sea water balance with the NAO index. We chose to use the station-based index for the estimation, since the coefficients of determination for it are slightly larger than those for the principal component.

Physically, a high NAO index means that the air pressure is higher than average over the southern part of the North Atlantic, or lower than average over the northern part. This kind of pressure gradient results in a prevailing westerly geostrophic wind, which forces water to enter through the Danish Straits into the Baltic Sea and also forces an east-west directed slope on the water surface within the Baltic Sea. This slope, correlating with the NAO index, causes the regression coefficients (Table 2) to vary with the tide gauge location, the largest coefficients being found at the closed ends of the Gulf of Bothnia and the Gulf of Finland (Johansson *et al.* 2003).

The NAO index may also correlate with the amount of precipitation over the Baltic Sea, as well as with river run-off into it (Vermeer *et al.* 1988). These factors may contribute to the general correlation between the NAO index and the sea level, although the exchange of water through the straits is the most important mechanism.

Scenarios for the NAO index

Seven different atmosphere–ocean general circulation models (AOGCMs) were used to obtain scenarios for the NAO index: HadCM3, CCCma-CGCM2, CSIRO-Mk2, CCSR/NIES, NCAR-PCM, ECHAM4/OPYC3 and GFDL-R30. For a more detailed description of the models, see Jylhä *et al.* (2004). The scenario data were obtained from the IPCC Data Distribution Centre, as monthly mean sea level pressure fields. Scenarios based on the SRES emission scenarios A1, A2, B1 and B2 were used. All the seven models provided the scenarios A2 and B2, but only CSIRO-Mk2 and CCSR/NIES also provided the scenarios A1 and B1.

As stated above, the NAO index was calculated as the leading principal component of the pressure field at sea level. The models reproduce qualitative properties of the anomaly field associated with the leading principal component (Fig. 4), but the location of the southern and northern pressure centres slightly varies from one model to another. The observed values of NAO during the 20th century are rather poorly reproduced by the models (Fig. 5), even though the range of the variation is of the right order.

Table 2. Correlation coefficients R , coefficients of determination R^2 and regression coefficients k_i and p_i for the relationship between the observed annual mean sea levels (detrended) at the Finnish tide gauges and two different versions of the winter (Dec.–Mar.) NAO index. The index denoted “Gibraltar–Iceland” is defined as a difference in the normalized air pressure anomalies at these sites (Jones *et al.* 1997). The one denoted “Principal component” is defined as the leading principal component obtained from an EOF analysis of the air pressure field over the North Atlantic (up to year 2000).

Tide gauge	Years of data	Gibraltar–Iceland			Principal component		
		R	R^2	k_i (cm)	R	R^2	p_i (cm)
Kemi	1923–2002	0.64	0.40	6.72	0.62	0.38	3.20
Oulu	1923–2002	0.62	0.38	6.60	0.58	0.34	3.14
Raahe	1923–2002	0.65	0.42	6.55	0.62	0.39	3.12
Pietarsaari	1922–2002	0.66	0.44	6.35	0.64	0.41	3.03
Vaasa	1922–2002	0.66	0.44	6.13	0.63	0.40	2.92
Kaskinen	1927–2002	0.67	0.44	6.23	0.63	0.39	2.95
Mäntyluoto	1925–2002	0.67	0.44	6.09	0.62	0.38	2.89
Rauma	1933–2002	0.68	0.46	6.08	0.61	0.37	2.91
Turku	1922–2002	0.66	0.44	6.07	0.62	0.38	2.90
Degerby	1924–2002	0.66	0.44	5.77	0.61	0.37	2.74
Hanko	1888–2002	0.61	0.37	5.66	0.60	0.36	2.75
Helsinki	1904–2002	0.61	0.38	6.09	0.60	0.36	2.89
Hamina	1929–2002	0.61	0.37	6.98	0.58	0.33	3.32

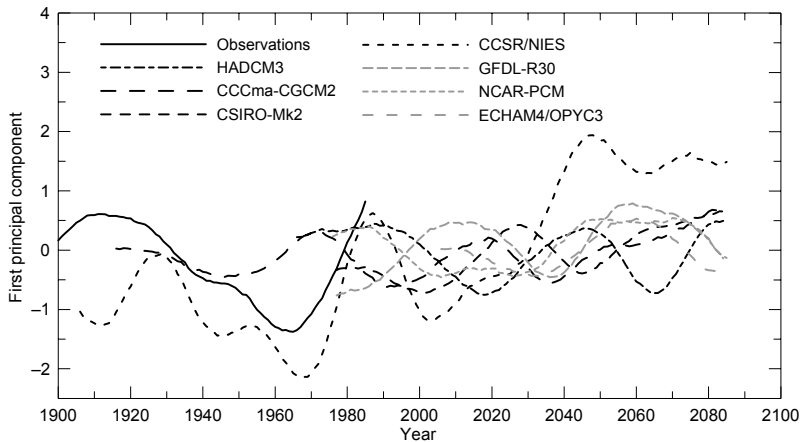


Fig. 5. Leading principal components obtained from an EOF analysis of the mean sea level pressure fields of different climate model runs for the SRES scenario A2. The EOF analysis was calculated from winter (Dec.–Mar.) mean pressure anomalies over an area extending from 20°N to 80°N and from 90°W to 30°E. Gaussian low-pass filtered time series given.

Even if the ability of the models to reliably predict the interdecadal variability of the leading principal component is questionable, we used the model-based trends in its amplitude in 1990–2100 as a basis for our sea level scenarios. The trends were scaled to correspond to the units of the station-based NAO index by a coefficient obtained from the mutual regression between the observed values of the two different indices. These scaled trends were then combined with the observed station-based index by fitting the trend line to coincide with the observed mean NAO index of the 20th century at the year 1990. To smooth out the year-to-year variations, 15-year moving averages were calculated (Fig. 6). We used the scenario A1 to represent the three scenarios A1FI, A1T and A1B, since no separate scenarios were available.

The trends are statistically significant in the scenarios A1 (at the 98% level) and A2 (at the 99.9% level), according to Student's *t*-test. The trends in the scenarios B1 and B2 are not statistically significant. However, the differences between emission scenarios are generally smaller than the scatter between different models. This is also the conclusion of the IPCC (2001), which states that consistency in the model results has not yet been achieved. While several models show an increase in the NAO index with increased greenhouse gases, this is not true for all of them.

Scenarios for the mean sea level on the Finnish coast

Combining the three factors presented above, the annual mean sea level $h_i(t)$ in a year t can be expressed as

$$h_i(t) = h_g(t) - u_{ai}t + k_i N(t) + l_i t + R_i + \varepsilon_{hi}(t) \quad (2)$$

where $h_g(t)$ is the global mean sea level, u_{ai} is the absolute land uplift rate, the water balance is represented by $k_i N(t)$, where $N(t)$ is the NAO, and k_i is the regression coefficient, obtained from a linear regression between the sea level and the NAO index (Table 2). The term $l_i t$ represents the possible linear trends in the sea level caused by effects other than land uplift, global mean sea level rise or trends in the NAO. The coefficient l_i thus contains the possible effect of changing salinity, for instance. The constant R_i is a site-dependent levelling constant, dependent on the choice of a bedrock-bound reference level of sea level values. The residual $\varepsilon_{hi}(t)$ represents any year-to-year sea level variations independent of the factors considered above. It has no trend, and its long-term mean vanishes.

A method for calculating an estimate for the long-term mean sea level can be derived from Eq. 2 (Johansson *et al.* 2003). Accordingly, the mean sea level estimates $w_i(t)$ for the 20th century as well as scenarios for the 21st century can be calculated using:

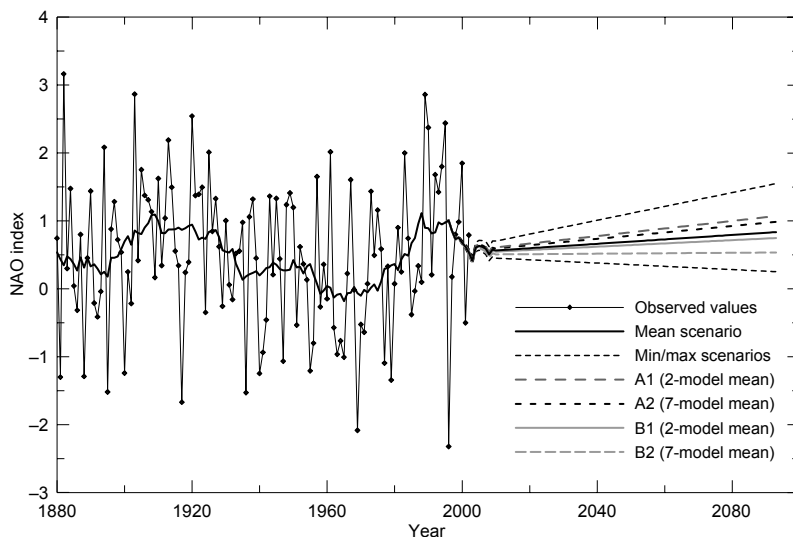


Fig. 6. Observed station-based NAO index (Jones *et al.* 1997), and estimated scenarios up to 2100. The minimum and maximum scenarios were obtained by calculating the 95% limits for each of the four trends separately, and by choosing the outermost limits thus obtained.

$$w_i(t) = h_g(t) - u'_{ai}t + k_i N_{ind}(t) + R'_i \quad (3)$$

There are some differences between $h_i(t)$ and $w_i(t)$. First, the NAO phenomenon itself, $N(t)$, is the physical process that affects both the observed pressure gradient, the NAO index $N_{ind}(t)$, and the sea level $h_i(t)$. The actual coefficients R_i and u_{ai} are represented by the estimates R'_i and u'_{ai} . These estimates are obtained from the observations with a linear fit, after correcting for the effect of the water balance.

Secondly, the difference between $N(t)$ and $N_{ind}(t)$ may contain a trend in time. This trend can be expressed with a term nt , where n is the slope of the trend and t is the year in question. This trend together with the trend $l_i t$, is left as an error term in the absolute land uplift estimate $u'_{ai} = u_{ai} - l_i + kn$. Assuming that the index $N_{ind}(t)$ truly represents the NAO, n can be estimated to be small. The coefficient l_i can also be estimated to be small, and thus u'_{ai} is an estimate of the actual land uplift rate (Johansson *et al.* 2003).

There are also large year-to-year variations in $N_{ind}(t)$, which would result in similar variability in the mean sea level estimate. In practice, a smooth mean sea level estimate — changing only a small amount from one year to the next — is often preferred. Thus, $w_i(t)$ was filtered with a 15-year moving average. It is also apparent that

the year-to-year variations of the NAO index are only partly correlated with the sea level, and thus their inclusion in an estimate of the mean sea level is not desirable.

Scenarios for the mean sea level $w_i(t)$ at selected tide gauges are presented in Fig. 7. The error limits consist of the uncertainties in the global mean sea level scenario, the NAO index scenario and the global mean sea level rise during the 20th century. The last one affects the scenarios for the 21st century through a resulting uncertainty in the absolute land uplift estimate u'_{ai} . The effects of each individual factor were combined in quadrature, following the usual practice for independent uncertainties. To represent the uncertainties of the global mean sea level rise, we chose the maximum and minimum scenarios, denoted “All SRES envelope including land-ice uncertainty” in Fig. 3. An example of the effect of uncertainties of individual factors on the mean sea level scenario is presented in Fig. 8.

Short-term sea level variability

Trends in short-term variability during the 20th century

To study the short-term, i.e. intra-annual varia-

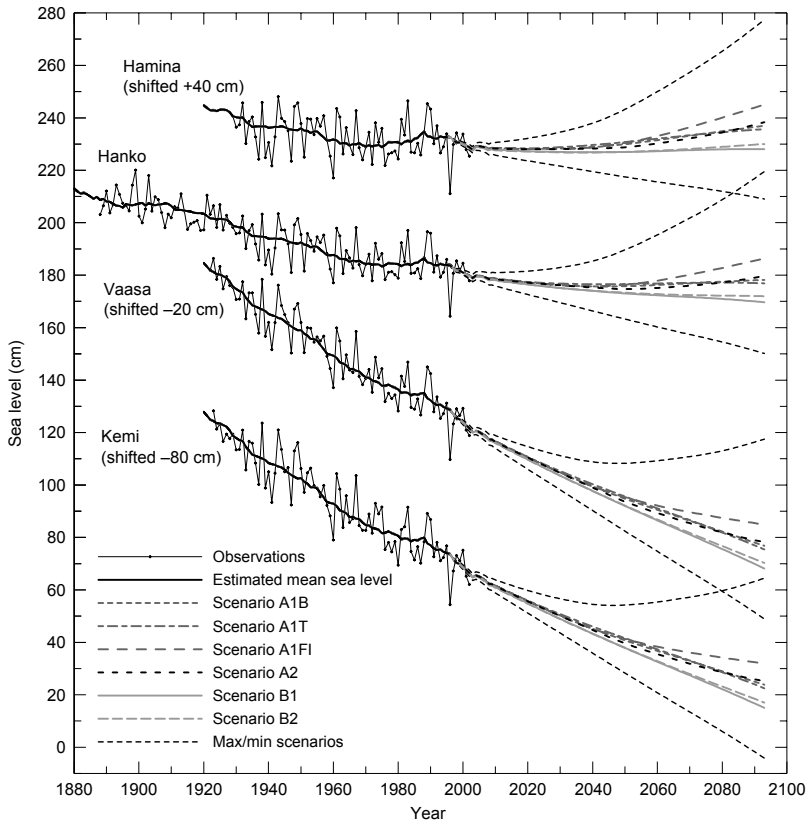


Fig. 7. Mean sea level scenarios at selected tide gauges, based on the different SRES emission scenarios, in relation to the bedrock-bound reference levels. The vertical scale is for Hanko, other stations have been shifted for clarity.

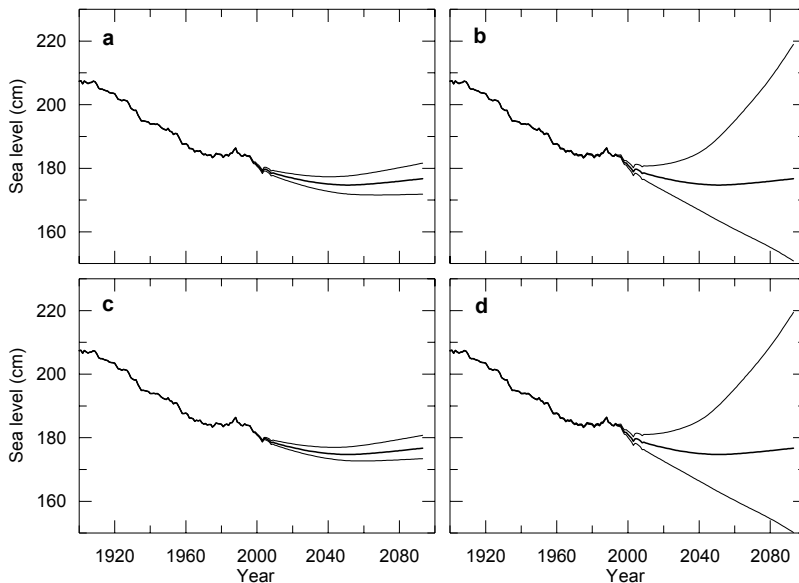


Fig. 8. Effect of the uncertainties in: (a) global mean sea level rise in the 20th century, (b) global mean sea level scenario in the 21st century, (c) the scenario of the NAO index in the 21st century and (d) all these together, to the scenario of the mean sea level at Hanko. The effect of each individual factor (a–c) is calculated assuming that the other factors get their central value.

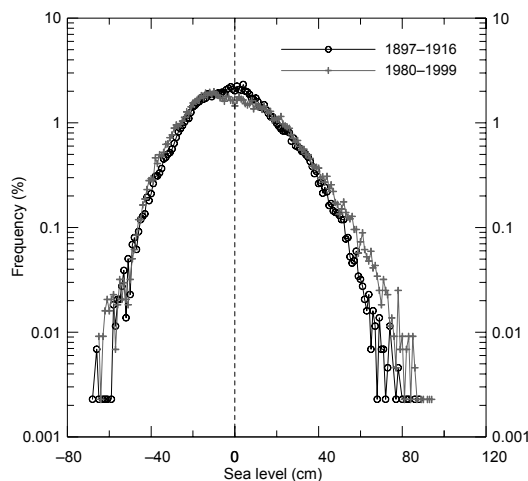


Fig. 9. Sea level frequency distributions at Hanko, calculated for two 20-year periods near the beginning and end of the 20th century. The sea level observations, at 4-hour intervals, were referenced to the observed annual mean sea levels. Thus, the distributions represent the intra-annual sea level variability. (Redrawn from Johansson *et al.* 2001.)

tions, it is necessary to separate them from the long-term variations. The simplest way is to subtract the observed annual mean sea levels from each 4-hourly observation, but this method removes a noticeable amount of the intra-annual variations. An alternative way is to subtract the mean sea level estimates $w_i(t)$ (Eq. 3). This excludes the variations caused by global mean sea level changes, land uplift and water balance on time scales longer than 15 years.

Johansson *et al.* (2001) presented a thorough study of the trends and changes observed in short-term sea level variability on the Finnish coast during the 20th century. The results of the study are summarized below, updated to include the most recent sea level data where appropriate.

Johansson *et al.* (2001) studied the short-term variations using the sea level frequency distributions, standard deviations at different time scales, as well as spectra. There are significant changes in these. The frequency distributions of sea level observations (Fig. 9) apparently changed in shape between the beginning and the end of the 20th century. The difference in the distributions for the years 1897–1916 and 1980–1999 is statistically significant at the 99.9% level.

Especially the probabilities for extremely

high sea level values increased. This is also apparent in the time series of annual maximum sea level values (Fig. 10). The positive linear trend — up to the year 2002 — is significant at the 99.9% level at Hanko, and at least at the 97% level at other Finnish tide gauges, excluding Kemi. However, the long-term changes in the annual maxima are not necessarily linear in nature. The 15-year moving average (Fig. 10) clearly shows that the maxima increased mainly during 1940–1980, and thereafter the trend seemed to turn to a decreasing one.

The annual standard deviation of the 4-hour interval observations (Fig. 11) is a simple measure of the intra-annual variability. A statistically significant positive trend (at the 95% level or higher, except at Kemi) is also evident in the annual standard deviations. However, as in the case of the annual maxima, the increasing trend turned to a decreasing one during the last decades of the 20th century.

A sea level amplitude spectrum was calculated from the time series of monthly mean sea levels at several of the Finnish tide gauges by Johansson *et al.* (2001). In these spectra, the annual cycle of the sea level is clearly visible as a distinct peak corresponding to the period of 12 months. The amplitude of this peak had a maximum around 1980, in accordance with the behaviour of the annual standard deviations.

Scenarios for short-term variability

In general, the sea level variability on time scales of a few days is controlled by local meteorological processes like air pressure and wind conditions. The water balance variations affect the sea level on time scales longer than about two weeks, contributing to the intra-annual variability.

The future behaviour of the short-term variability can be roughly estimated by a linear extrapolation of the 20th century trends of annual maxima and standard deviations. This method predicts an increasing variability during the 21st century. This may be an overestimate, however, since the increasing trends of the 20th century seemed already to turn to decreasing ones during the last decades of the century (Figs. 10 and 11). The method of extrapolating a positive linear

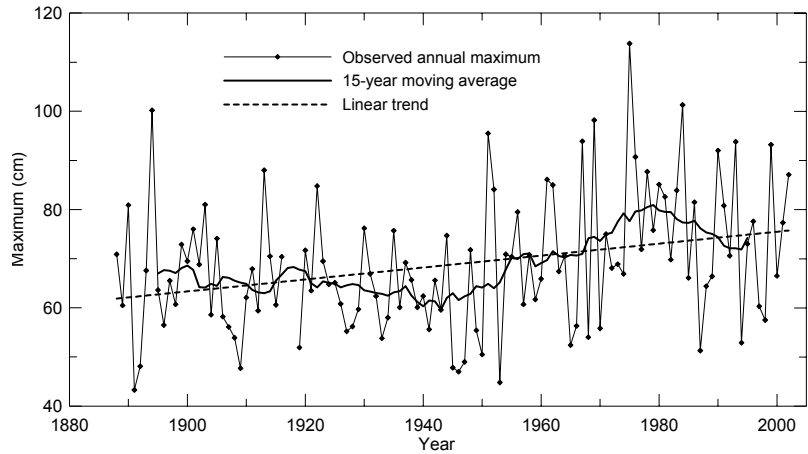


Fig. 10. Annual maximum sea levels observed at Hanko, in relation to the annual mean sea levels.

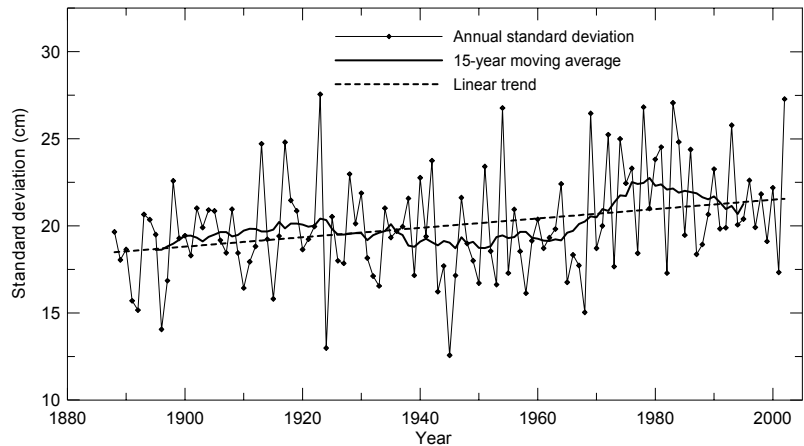


Fig. 11. Annual standard deviation of 4-hourly sea level observations at Hanko.

trend yields an upper limit for the future behaviour of the short-term sea level variations.

Combining the scenarios of the mean sea level and the short-term variability yields important information about the occurrence of extreme sea levels in the future. As an example of such estimation, we calculated the probabilities for certain high sea levels at Hanko for several years during the 21st century (Table 3). The SRES scenario A2 was chosen.

The probabilities were calculated by combining the probability distributions of the long-term mean sea level and the short-term variability. To be able to do this, we constructed a probability distribution for the mean sea level scenarios. We considered the maximum and minimum scenarios (Fig. 7) to represent the 5% and 95% probabilities, respectively, and a 50% probability was attached to the mean sea level scenario based on

the scenario A2. A Weibull-type distribution was fitted to these three points for each year.

As the interest was on extremely high sea levels, the probability distribution for the short-term variability was based on the observed frequency distribution of the monthly maximum sea levels. This distribution was extrapolated to the future by applying a correction obtained from the linear trends in the observed monthly maximum sea levels, separately for each month. To estimate probabilities for extremely rare sea level values, the observed frequency distribution was extrapolated to higher sea level values by fitting an exponential distribution. This distribution was then combined with the mean sea level distribution to obtain a combined probability, which takes into account both the short-term variability and the uncertainty in the mean sea level scenarios.

Discussion

Uncertainties in the mean sea level scenarios

The different SRES emission scenarios result in slightly different sea level scenarios on the Finnish coasts. In 2093, the difference between the highest (A1FI) and lowest (B1) scenario amounts to approximately 20 cm. Still, this is much smaller than the difference of 70 cm between the minimum and maximum scenarios. This uncertainty of 70 cm results from uncertainties in the three factors discussed determining the long-term mean sea level.

The uncertainty in the global mean sea level rise is the dominant source of uncertainty in the scenarios (Fig. 8). In 2005, the scenarios corresponding to the minimum and maximum global mean sea level rise differ by only 3 cm at every tide gauge. The corresponding difference caused by the minimum and maximum NAO scenarios is only 1 cm, and the effect of the inaccuracy in the 20th century global mean sea level rise estimate is also 1 cm. By 2093, the scenarios based on the minimum and maximum global mean sea level rise differ by 67–68 cm, while the scenarios based on the different NAO scenarios differ by only 7–9 cm, and the scenarios based on the different 20th century global mean sea level rise estimates differ by 9–10 cm.

The global mean sea level scenarios of the IPCC (2001) do not consider the possible contribution from the collapse of the Antarctic ice sheets. According to Vaughan and Spouge (2002), there is a 5% probability of the collapse

of the West Antarctic Ice Sheet resulting into at least 10 mm yr⁻¹ sea level rise within 200 years. Such rise would raise the maximum sea level scenarios at 2100 by about one meter. This would be a dominating effect in the global mean sea level scenarios, and would change our results significantly. As such an event is unlikely, we have chosen not to include it in our scenarios, in accordance with a similar decision of the IPCC.

The climate models do not yet give reliable scenarios for the NAO index in the 21st century. In this study, we used an approximation based on the trends of the modelled NAO index. The trends behave in a consistent way — the increasing trends for the A scenarios being stronger than those for the B scenarios.

The ability of the models to describe the NAO index is analysed in more detail in several studies. Osborn *et al.* (1999) used the model HadCM2 and found a decreasing trend during the next 100 years. Paeth *et al.* (1999) used the models ECHAM3/LSG and ECHAM4/OPYC3, in which the index would stabilize in a positive state during the 21st century. Ulbrich and Christoph (1999) also found an increasing trend, based on the model ECHAM4/OPYC3. These studies, however, were not based on the SRES emission scenarios utilised in our study. Other studies related to the NAO scenarios include those of Shindell *et al.* (2001) and Gillett *et al.* (2002).

The scenarios presented in this study rely on the assumption that the correlation between the NAO index and the water balance does not change its nature in the future. This might not be the case, however, since the correlation has changed in the past. The correlation is generally weaker for the 19th century than for the 20th century (Andersson 2002, Johansson *et al.* 2003). This might be caused by changes in the underlying processes, although inaccuracies in the earlier observations of both the sea level and the air pressure are a more likely explanation.

Table 3. Probabilities for sea level at Hanko exceeding certain levels in relation to the mean sea level of 2000, based on the SRES scenario A2. The probabilities are expressed as the number of monthly maxima exceeding the limit in a certain year, the maximum probability thus being 12 yr⁻¹.

Year	Probability (yr ⁻¹) of sea level exceeding			
	100 cm	110 cm	120 cm	130 cm
2000	5.1×10^{-2}	1.6×10^{-2}	9.0×10^{-3}	2.1×10^{-4}
2020	3.9×10^{-2}	1.4×10^{-2}	4.4×10^{-3}	1.8×10^{-4}
2040	4.1×10^{-2}	1.4×10^{-2}	4.6×10^{-3}	4.7×10^{-4}
2060	7.7×10^{-2}	2.9×10^{-2}	9.8×10^{-3}	2.8×10^{-3}

Uncertainties in the scenarios of short-term variability

The probabilities for certain extremely high sea levels slightly decrease during the next few decades in the scenario A2 at Hanko, according

to the results in Table 3. After 2020, however, the probabilities tend to rise. This is caused by the properties of the mean sea level scenario A2 (Fig. 7), which indicate that the mean sea level at Hanko will fall up to the 2040s and start to rise thereafter. In addition to this, the probabilities are affected by the extrapolated increasing short-term variability, as well as the widening of the uncertainty limits of the mean sea level scenario — resulting in a widening probability distribution. Both latter factors tend to increase the probabilities of high sea levels.

The probabilities (Table 3) are more likely to be overestimates than underestimates, since the extrapolation of the observed, increasing trend of short-term variability is likely to overestimate the variability in the future. Especially in the latter half of the 21st century, this might lead to significant overestimation.

Another source of uncertainty in the probabilities is the extrapolation of the frequency distributions to extremely high sea level values. Since the available time series of sea level observations at Hanko is only 115 years long, extreme values with frequencies less than about 10^{-2} yr^{-1} have to be extrapolated.

Practical applications

Estimates of the present and future behaviour of the sea level are important for practical purposes like coastal construction, planning, safety estimation and navigation. At FIMR, an estimate of the mean sea level, called the “theoretical mean sea level”, has traditionally been established for a few years ahead (Fig. 2). This estimate has been based on the assumption of a linear behaviour of the mean sea level with time. The possibility of accelerated sea level rise requires a more general definition of the concept, and therefore the theoretical mean sea level is now understood as a time-dependent expectation value of the annual mean sea level. The sea level scenarios presented in this study allow the establishment of a theoretical mean sea level that takes into account the accelerating global mean sea level rise as well as the effect of the water balance.

The theoretical mean sea level is an official estimate used for planning and administra-

tive purposes, and as such, it should be kept unchanged once established. Thus, the establishment of the theoretical mean sea level to a distant future is not feasible. Coastal construction and planning usually deals with structures with a lifetime of several decades, and thus estimates of the behaviour of the sea level in the distant future are also needed. These estimates, however, are updated when a better understanding of the sea level behaviour and scenarios is achieved.

The probabilities for the occurrence of extremely high sea levels are also often of interest in connection with coastal construction activities and safety estimation. Thus, estimates like the one presented (Table 3) are needed. In such cases, an overestimate of the probability of a high sea level is usually a safer choice. Thus, it is acceptable to use a method like that suggested above, where the extrapolation of the 20th century trends is likely to result in an overestimate of the future variability. However, an overestimate and resulting over-protection may lead to increased design costs. In such projections, the risks, the consequences of possible flooding, and the design costs have to be assessed case by case to make an acceptable compromise.

Conclusions

In the Gulf of Finland, the past declining trend of the mean sea level will probably not continue in the future, because the accelerating rise in the global mean sea level will balance the land uplift. This is the case according to all the six emission scenarios studied — A1FI, A1B, A1T, A2, B1 and B2. The A scenarios predict a rise of 10–20 cm up to the 2090s relative to the present-day mean sea level. The B scenarios predict the mean sea level to stay at an approximately constant level during the 21st century, with changes of only a few centimetres.

The uncertainties are large, however, amounting to several tens of centimetres at the end of the 21st century. The maximum scenario predicts a sea level rise of 50 cm at Hamina, in the eastern part of the Gulf of Finland, while the minimum scenario results in a still falling mean sea level.

In the Gulf of Bothnia, the stronger land uplift rate results in probable fall of the mean sea level

in the future according to all the six emission scenarios. The uncertainties are of the same order as those for the Gulf of Finland. According to the maximum scenario, the mean sea level will start to rise after the middle of the 21st century even in the area of the strongest land uplift, at Vaasa.

The short-term variability of the sea level increased during the 20th century; especially the frequencies of extremely high sea level values increased. There is no evidence, however, that this increase would continue in the 21st century, since the trend turned to a decreasing one during the last two decades of the 20th century. Rough estimates of short-term sea level variability in the future were calculated by extrapolating the observed trend in the 20th century.

Acknowledgements: We thank Kirsti Jylhä and Heikki Tuomenvirta from the Finnish Meteorological Institute for cooperation in the estimation of the future NAO scenario, and Timothy Carter from the Finnish Environment Institute for valuable comments and suggestions on the manuscript. The IPCC Data Distribution Centre is acknowledged for providing the climate model data. This study was a part of the project FIGARE/FINSKEN, and was financially supported by the Academy of Finland and the Finnish Ministry of Transport and Communications.

References

- Andersson H.C. 2002. Influence of long-term regional and large-scale atmospheric circulation on the Baltic sea level. *Tellus* 54A: 76–88.
- Basnett T.A. & Parker D.E. 1997. *Development of the Global Mean Sea Level Pressure Data Set GMSLP2*. Climatic Research Technical Note No. 79, Hadley Centre, Meteorological Office, Bracknell.
- Carter T.R., Fronzek S. & Bärlund I. 2004. FINSKEN: a framework for developing consistent global change scenarios for Finland in the 21st century. *Boreal Env. Res.* 9: 91–107.
- Gillett N.P., Allen M.R., McDonald R.E., Senior C.A., Shindell D.T. & Schmidt G.A. 2002. How linear is the Arctic Oscillation response to greenhouse gases? *J. Geophys. Res.* 107 No. D3: 1–1–1–7.
- Gornitz V. 1995. Monitoring sea level changes. *Climatic Change* 31: 515–544.
- IPCC 2001. *Climate change 2001: The scientific basis. Contribution of Working Group I to the Third Assessment Report of the Intergovernmental Panel on Climate Change*. Cambridge University Press, Cambridge, United Kingdom and New York, NY, USA.
- Johansson M., Boman H., Kahma K.K. & Launiainen J. 2001. Trends in sea level variability in the Baltic Sea. *Boreal Env. Res.* 6: 159–179.
- Johansson M.M., Kahma K.K. & Boman H. 2003. An Improved Estimate for the Long-Term Mean Sea Level on the Finnish Coast. *Geophysica* 39(1–2): 51–73.
- Jones P.D., Jonsson T. & Wheeler D. 1997. Extension to the North Atlantic Oscillation using early instrumental pressure observations from Gibraltar and south-west Iceland. *Int. J. Climatol.* 17: 1433–1450.
- Jylhä K., Tuomenvirta H. & Ruosteenoja K. 2004. Climate change projections for Finland during the 21st century. *Boreal Env. Res.* 9: 127–152.
- Kahma K. 1999. Atlantin ilmanpaine vaikuttaa Itämereen [NAO is reflected in the Baltic sea level]. *Finnish Institute of Marine Research, Annual Report 1999*. [In Finnish with English summary].
- Lisitzin E. 1964. Contribution to the knowledge of land uplift along the Finnish coast. *Fennia* 89(4): 1–22.
- Lisitzin E. 1966. Mean sea level heights and elevation systems in Finland. *Societas Scientiarum Fennica, Commentationes Physico-Mathematica* 32(4): 1–14.
- Nakićenović N., Alcamo J., Davis G., de Vries B., Fenhann J., Gaffin S., Gregory K., Grübler A., Jung T.Y., Kram T., La Rovere E.L., Michaelis L., Mori S., Morita T., Pepper W., Pitcher H., Price L., Raihi K., Roehrl A., Rogner H.-H., Sankovski A., Schlesinger M., Shukla P., Smith S., Swart R., van Rooijen S., Victor N. & Dadi Z. 2000. *Emissions scenarios. A special report of Working Group III of the Intergovernmental Panel on Climate Change*. Cambridge University Press.
- Osborn T.J., Briffa K.R., Tett S.F.B., Jones P.D. & Trigo R.M. 1999. Evaluation of the North Atlantic Oscillation as simulated by a coupled climate model. *Climate Dynamics* 15: 685–702.
- Paeth H., Hense A., Glowienka-Hense R., Voss R. & Cubasch U. 1999. The North Atlantic Oscillation as an indicator for greenhouse-gas induced regional climate change. *Climate Dynamics* 15: 953–960.
- Shindell D.T., Schmidt G.A., Miller R.L. & Rind D. 2001. Northern Hemisphere winter climate response to greenhouse gas, ozone, solar, and volcanic forcing. *J. Geophys. Res.* 106: 7193–7210.
- Thompson D.W.J. & Wallace J.M. 2000. Annular modes in the Extratropical Circulation. Part I: Month-to-month variability. *Journal of Climate* 13: 1000–1016.
- Ulbrich U. & Christoph M. 1999. A shift of the NAO and increasing storm track activity over Europe due to anthropogenic greenhouse gas forcing. *Climate Dynamics* 15: 551–559.
- Vaughan D.G. & Spouge J.R. 2002. Risk estimation of collapse of the West Antarctic Ice Sheet. *Climatic Change* 52: 65–91.
- Vermeer M., Kakkuri J., Mälkki P., Boman H., Kahma K.K. & Leppäranta M. 1988. Land uplift and sea level variability spectrum using fully measured monthly means of tide gauge readings. *Finnish Marine Research* 256: 1–75.